

Electronic friction in the presence of strong intra-atomic correlations for atoms moving near metal surfaces

M. Plihal and David C. Langreth

Department of Physics and Astronomy, Rutgers University, Piscataway, New Jersey 08855-0849

(Received 30 December 1998)

We present a theory of energy transfer between metal surfaces and atoms moving near the surface. We investigate the effects of the intra-atomic electron correlations on the nonadiabatic energy transfer, related to electronic friction. Two special cases of atoms moving (a) parallel and (b) perpendicular to the surface are discussed. Analytic expression is derived for the energy transfer of an interacting system with atoms moving parallel to a smooth surface with finite velocity. In the Kondo regime, we find substantial enhancement and strong temperature dependence of the friction coefficient. The maximum effect occurs when the substrate electronic temperature is of the order of the Kondo temperature, T_K . The interference between the parallel and perpendicular directions of motion is small for all experimentally relevant conditions. However, the parallel component of velocity affects the energy transfer that one would find under the conditions of perpendicular motion. [S0163-1829(99)14627-7]

I. INTRODUCTION

One of the interesting recent developments in surface science has been the direct spectroscopic observation of the Kondo resonance in the electronic structure of magnetic atoms chemisorbed on metal surfaces. Two independent experiments were performed using low-temperature scanning tunneling microscopy (STM) with atomic-scale resolution on two different atom-metal systems Co/Au(111) (Ref. 1) and Ce/Ag(111) (Ref. 2)—well known to be Kondo impurity alloys with high Kondo temperature $T_K \sim 300$ K and ~ 1000 K, respectively. The observed feature appears as a narrow resonance at the Fermi energy ϵ_F of the host metal and is spatially limited to the vicinity of the adsorbed magnetic atoms. The inferred Kondo temperatures are 80 K for Co/Au(111) and 50 K for Ce/Ag(111). We note, however, that alternative explanation for the resonance cannot be ruled out at this time and a truly unambiguous conclusion will require further studies of the temperature and magnetic field dependence.

The Kondo resonance is a manifestation of many-body interactions between the metal electrons and the local impurity moment. It forms as a consequence of spin-flip scattering of the conduction electrons at the Fermi surface from the uncompensated spin of the magnetic atom. This leads to a screening of the local spin at low temperatures and the formation of a singlet many-body ground state. Physical consequences of the Kondo resonance are widely discussed in the context of dilute magnetic alloys,³ where it is known to give rise to anomalous transport properties—the Kondo effect.

However, very little is currently known about its possible effects at surfaces. Fundamentally important questions, which are not encountered in the problem of magnetic impurities in metals, emerge in the context of surface physics. First of all, it is unclear what, if any, effects the intra-atomic Coulomb repulsion can have in surface processes. Second, the surface problem exhibits the interplay between nonequilibrium and many-body effects. This is because the atoms

near the surface are free to move and thus represent a localized dynamic perturbation of the Fermi sea. The response to such a perturbation is never adiabatic and the system exhibits anomalous behavior.⁴ The nonadiabatic effects can further be enhanced by the Coulomb interaction.⁵

One of the most fundamental surface processes is the charge transfer between metal surfaces and ions adsorbed on or scattering from the surface. The intra-atomic correlations were predicted to cause strong temperature and energy dependence of ion yields in scattering experiments.^{5,6} The central question addressed in this paper is how the Coulomb repulsion affects electronic friction. Its knowledge is important because the nature of many surface processes is determined by how energy flows between the various degrees of freedom involved. For example, electronic friction is directly related to activation rates in desorption induced by electronic transitions (DIET, DIMET), bond breaking, etc.

Two conditions must be satisfied for the Coulomb repulsion to have significant physical consequences in real processes. First of all, the intra-atomic correlations must have a considerable effect on the electron-hole mechanism and must modify the nonadiabatic energy transfer. Indeed, large effects have already been predicted under certain conditions.⁷ However, this by itself is not sufficient because other channels for energy transfer always participate and frequently dominate in the processes. Therefore, the conclusions from our theory, which deals only with the electronic degrees of freedom, will be relevant for processes which are activated or otherwise dominated by the electronic mechanism. We devote the next few paragraphs to this issue.

The importance of electronic involvement in various atomic and molecular processes at metal surfaces has been demonstrated experimentally in recent years. The idea of electron activated processes was invoked a long time ago by Bohnen *et al.*⁸ in connection with catalytic reactions of H atoms on metal surfaces. They view the chemical reaction as a Brownian motion of the system on its reaction trajectory. The small system, the H atom in this case, is assumed to be in contact with the electron heat bath of the metal. The reaction rate is then controlled by the dissipative part (electronic

friction coefficient η) of the interaction between the reagent and the degrees of freedom of the heat bath, formally expressed in terms of the force autocorrelation function. The electronic friction of atoms near metal surfaces was later considered in detail by Nourtier.⁹

The electron-hole mechanism has been suggested by Persson and Persson¹⁰ as a determining factor in vibrational lifetimes of CO adsorbed on Cu(100). Infrared reflection spectroscopic studies of the system indeed showed very little temperature dependence of the linewidths, thus lending strong support to the idea of electronic involvement.^{11,12} Studies of vibrational line shapes confirmed this view.^{13,14} In addition, molecular-dynamics simulations of vibrational damping of the different CO/Cu(100) vibrational modes,¹⁵ and finite cluster modeling of the C-O stretch mode lifetimes,^{16,17} all found the electronic mechanism very important.

The availability of time-resolved experimental techniques with resolutions on femtosecond time scales makes it possible to study the dynamics of the energy flow between individual degrees of freedom involved in the process. For instance, recent femtosecond pulse laser experiments^{18,19} carried out on CO/Cu(111) and NO/Pd(111) systems come close to being able to control the lattice and electronic temperatures independently. Using sequences of two laser pulses with different time separations, the desorption times were found to be less than 1 ps—too short to be explained by the conventional thermal desorption. The lattice temperature is too low on this time scale to explain the high desorption rates by the traditional thermal desorption. Furthermore, the desorption yield is a highly nonlinear function of the laser fluence. These two characteristics strongly indicate that the desorption is induced by multiple electronic transitions (DIMET) of hot substrate electrons in and out of the negative ion resonance ($2\pi^*$).

A different conceptual framework for desorption mediated by a single highly nonequilibrium hot electron (DIET) was used by Gadzuk *et al.*²⁰ to explain earlier desorption experiments for NO/Pt(111) system induced by nanosecond laser pulses of significantly smaller fluence ($\sim 500 \mu\text{J}/\text{cm}^2$). The analysis of the final-state distribution as a function of the photon energies and the linear dependence of the desorption yield indeed suggest that an excitation by a single photoelectron into the excited potential energy surface (PES) takes place.

Closely related to DIMET is the process of vibrational heating invoked by Gao *et al.*²¹ and Walkup *et al.*²² as the mechanism involved in the atom transfer via STM (atomic switch)²³ and in STM assisted single molecule dissociation at metal surfaces.²⁴ The common feature of this set of problems is a potential-barrier crossing or bond breaking through vibrational activation. At small tunneling currents, the activation is dominated by (coherent) inelastic scattering of a single tunneling electron. At larger tunneling currents, the activation process involves many cycles of competing processes. The vibrational energy gains achieved via (incoherent) inelastic scatterings of the tunneling electrons are accompanied by vibrational deexcitations via electron-hole and phonon excitations in the metal.²⁵

Another area where electronic friction seems to play an important role is the sliding friction²⁶ in the systems studied

by Krim *et al.*²⁷ As of now, however, the question of the electron contribution to sliding friction is not fully resolved. Our work is not directly related to these experiments since we are dealing with electronic friction of single atoms and molecules.

The conclusions drawn from the above experiments show that many surface processes of great importance are electronically activated. A variety of theoretical approaches has been employed in their study. A common feature appearing in these processes is the presence of an atom-induced resonance close to the Fermi level which dominates in the dynamics. In the laser-induced desorption experiments, hot electron excitations into this level result in the Franck-Condon process. In the STM experiments, the electron tunneling through the resonance leads to vibrational heating. The importance of electronic friction derives not only from the fact that it causes the damping of ionic translational, vibrational, or rotational motion, but also because it is directly related to the activation rate of many surface processes. Hence, it enters the theoretical description of a large number of phenomena.

The spin degrees of freedom are usually neglected in the description, or they are included trivially as a degeneracy factor in the appropriate sums. Such theories neglect the potentially important effects of Coulomb correlations. The nonadiabatic coupling between different potential surfaces, which gives rise to electronic friction and is essential in the activation process, can be strongly influenced by the intra-atomic Coulomb repulsion especially in open-shell atoms. For example, the Kondo or mixed-valent resonances could form in atom-metal complexes with appropriate combination of work functions ϕ and ionization potentials (or affinity levels) of the atom. In a previous paper,⁷ hereafter referred to as I, we studied, in detail, the electronic friction in the presence of strong intra-atomic Coulomb interaction for adparticles whose motion is normal to the surface. We found the nonadiabatic energy transfer is affected both qualitatively and quantitatively by the presence of the Coulomb repulsion.

In this paper, we study the electronic friction for atoms with fully two-dimensional motion. One question asked by this study is whether the parallel component introduces significant interference effects with the perpendicular motion that could destroy the correlation effects occurring in purely perpendicular direction desorption? The conclusions of our study indicate that the intra-adsorbate Coulomb correlations could significantly enhance the activation rates of magnetic adsorbates with the Kondo scale. The most promising among these processes is the manipulation of atoms with STM tip. This problem is now under investigation.

We present the conceptual and theoretical framework in the following section. In Sec. IV, we discuss the results of our numerical calculations and we summarize our findings in Sec. V. Certain theoretical details are presented in Appendices A and B.

II. THEORETICAL DESCRIPTION

We consider a single atom or molecule in the presence of a smooth surface of a simple metal. We want to emphasize that molecules with appropriate electronic structure are covered by our theory. Most of the formulation, as well as con-

clusions, presented here are general enough to be applicable to different phenomena discussed in the Introduction. For this reason, the reader is free to interchange the frequently used words ‘‘atom’’ or ‘‘ion’’ for ‘‘adsorbate’’ or ‘‘projectile’’ as it applies.

We define a vector $\vec{R} = (\vec{R}_{\parallel}, Z)$, which determines the time-dependent position of the atom with respect to a reference point on the surface, Z being the distance from the surface and \vec{R}_{\parallel} being the lateral displacement from a reference point on the surface. We further assume that a single N -degenerate atom-induced resonance near the Fermi level ϵ_F dominates the dynamics. The degeneracy is at least 2 due to spin, but could be higher.

A. Basic model

We describe the atom-metal electronic system by a time-dependent Hamiltonian,

$$H(\vec{R}) = \sum_a \epsilon_a(Z) c_a^\dagger c_a + H_{\text{int}}[Z, c_a^\dagger c_a] + \sum_{ak} \epsilon_k c_{ka}^\dagger c_{ka} + \sum_{ak} \{V_{a,\vec{k},\vec{Q}}(\vec{R}) c_{ka}^\dagger c_a + \text{H.c.}\}, \quad (2.1)$$

where \vec{Q} is the electronic momentum shift associated with the projectile velocity \vec{R} . In atomic units adopted throughout this paper, $\vec{Q} = \vec{v} = \dot{\vec{R}}$. The time dependence of the ϵ_a , $V_{a,\vec{k},\vec{Q}}$, and H_{int} enters parametrically through the spatial coordinate R . The time dependence of the many-body interaction term H_{int} has its origin in the screening of the intra-atomic repulsion by the conduction electrons in the metal. We also note that, for general motion, \vec{Q} itself is a function of time. We will specify the time dependence explicitly where necessary, but omit it where no confusion can arise.

The first term describes the relevant electronic structure of the atom in the presence of the surface. The atomic levels $\epsilon_a(Z)$ are given by their value for infinite atom-surface separation ϵ_∞ shifted by the interaction $V_s(Z)$ with the metal surface,

$$\epsilon_a(Z) = \epsilon_\infty + V_s(Z). \quad (2.2)$$

The second term in Eq. (2.1) takes into account the intra-atomic many-body interactions. The operator c_a^\dagger creates an electron in the atomic orbital a . The index a is shorthand for the complete set of quantum numbers specifying the N -degenerate atomic levels. We assume that it corresponds to symmetries which are shared with the conduction electrons including at least the conservation of spin and possibly orbital symmetries, such as the reflection through planes perpendicular to the surface. Therefore, a can be used as a quantum number for the substrate electrons, as well. The operator c_{ka}^\dagger creates a conduction electron in the indicated symmetry state. The substrate band energies ϵ_k depend on the wave vector k only. The third term in Eq. (2.1) thus describes the electronic structure of the metal.

The last term in the Hamiltonian (2.1) provides for the electron hopping between the atom and the metal. It incorporates the effects of atomic motion in a nontrivial fashion as

discussed below. We first write the matrix element for an atom at rest a distance Z from a metal surface,

$$V_{a,\vec{k}}^{(S)}(Z) = \int d^3r \psi_{\vec{k}}^*(\vec{r}) v(\vec{x}_{\parallel}, z-Z) \phi_a(\vec{x}_{\parallel}, z-Z). \quad (2.3)$$

Here $\phi_a(\vec{r})$ is the wave function for the atomic level a . This is the usual ‘‘static’’ matrix element describing the electron scattering in and out of the atomic levels. In the case of a moving atom, the matrix element becomes

$$V_{a,\vec{k},\vec{Q}}(\vec{R}(t)) = \int d^3r \psi_{\vec{k}}^*(\vec{r}) v(\vec{x}_{\parallel}, z-Z) \phi'_a(\vec{r}), \quad (2.4)$$

where now $\phi'_a(\vec{r})$ is the wave function for the atomic level a as viewed from the metal surface. This wave function is related through a coordinate transformation to the solution $[\phi_a(\vec{r} - \vec{R})]$ in the frame in which the atom is at rest,

$$\phi'_a(\vec{r}) = \phi_a[\vec{r} - \vec{R}(t)] \exp \left[i \vec{Q}(t) \cdot [\vec{r} - \vec{R}(t)] + \frac{i}{2} \int^t Q^2(\tau) d\tau \right], \quad (2.5)$$

where $\vec{Q}(t)$ is the electronic momentum shift due to the atom motion at time t . The time-varying magnitude and phase of the matrix element each have qualitatively different effects and it is useful to exhibit them explicitly. We assume that the surface is uncorrugated in the regions important to the matrix element. Then the Bloch state $\psi_{\vec{k}}$ is of the form $\psi_{\vec{k}} = u_{k_z}(z) e^{i\vec{k}_{\parallel} \cdot \vec{x}_{\parallel}}$, and the metal-atom interaction $V_s(z)$ only depends on the distance from the surface. Then the matrix element can be written

$$V_{a,\vec{k},\vec{Q}}(\vec{R}) = V_{a,\vec{k} - \vec{Q}}(Z) e^{i\theta_{\vec{k},\vec{Q}}(\vec{R})}, \quad (2.6)$$

where

$$V_{a,\vec{k} - \vec{Q}}(Z) = \int d^3r \psi_{\vec{k} - \vec{Q}}^*(\vec{x}_{\parallel}, z+Z) v(\vec{r}) \phi_a(\vec{r}) \equiv \int dz h_{\vec{k} - \vec{Q}}(z, Z) \quad (2.7)$$

only contains the effects of parallel velocity and may always be taken real for the uncorrugated surface considered here. In the rest of this paper, we choose the coordinate origin so that $V_{a,\vec{k} - \vec{Q}}(Z)$ is indeed real. The phase θ has contributions from both parallel and perpendicular motion and is given by

$$\theta_{\vec{k},\vec{Q}}(\vec{R}) = -\vec{k} \cdot \vec{R}_{\parallel} + \frac{1}{2} \int^t Q^2(\tau) d\tau + \bar{\theta}_{\vec{k},\vec{Q}}(Z), \quad (2.8)$$

with

$$\bar{\theta}_{\vec{k},\vec{Q}}(Z) = Q_z \frac{\int dz z h_{\vec{k} - \vec{Q}}(z, Z)}{\int dz h_{\vec{k} - \vec{Q}}(z, Z)} + \dots \quad (2.9)$$

We refer the reader to Ref. 28 for detailed discussion of the assumptions and approximations involved here. We define the adiabatic rate $\Gamma_a(\omega, Z)$ for electronic tunneling between the metal and atomic states,

$$\Gamma_a(\omega, Z) = 2\pi \sum_k [V_{a,k}(Z)]^2 \delta(\omega - \epsilon_k). \quad (2.10)$$

We need to comment on the question of nuclear motion which is absent in the Hamiltonian (2.1). The position and velocity of the atom enters the problem implicitly through the parametrization of $V_{a,k}^{(S)}(\vec{R})$ and $\epsilon_a(Z)$. A full calculation (e.g., molecular dynamics) would proceed from a given initial configuration of the nuclear and electronic degrees of freedom, which specifies the forces acting on the nuclear motion. Classical equations of motion are then solved in a self-consistent manner by recalculating the forces at each step of the calculation. The generalized electronic friction coefficient $\eta(\vec{R})$ studied in this work is related to the electronic component of the dissipative forces, which enter the equations of motion.

B. Energy transfer

We now turn to the description of the nonadiabatic energy transfer. The details of the theoretical approach are discussed elsewhere.²⁸ Here, we generalize the theory to include the most general trajectory of the atom. The rate of adding (removing) energy to the system described by Eq. (2.1) is given by⁷

$$\begin{aligned} \dot{E}(\vec{R}, \vec{Q}) &= \sum_a \dot{\epsilon}_a(Z) \mathcal{G}_{a,\vec{Q}}^<(t, t) \\ &+ \sum_{ka} \{ \dot{V}_{a,k,\vec{Q}}(\vec{R}) \mathcal{G}_{a,k,\vec{Q}}^<(t, t) + \text{H.c.} \}, \end{aligned} \quad (2.11)$$

valid for general motion. Here, $\mathcal{G}_{a,\vec{Q}}^<(t, t') = \langle c_a^\dagger(t') c_a(t) \rangle_{\vec{Q}}$ and $\mathcal{G}_{a,k,\vec{Q}}^<(t, t') = \langle c_{ka}^\dagger(t') c_a(t) \rangle_{\vec{Q}}$. The subscript \vec{Q} indicates nonthermal, velocity-dependent average. In writing Eq. (2.11), we neglected the contribution from the time dependence in $H_{\text{int}}[Z]$.

The nonadiabatic part, $\dot{E}_{\text{n.a.}}(\vec{R}, \vec{Q})$, of the energy transfer (2.11) determines the dissipative energy flow from various nuclear degrees of freedom. The kinetic energy is the only form of energy involved if the projectile (adsorbate) is structureless. However, different degrees of freedom—such as rotations and vibrations—participate in general. It is not the purpose of this work to study the details of the final energy distribution, although its knowledge is certainly very important for the dynamics of many processes. The expression (2.11) also describes the energy flow in the opposite direction, i.e., from the system of hot electrons into the nuclear degrees of freedom. This follows from the fluctuation-dissipation theorem.

We define the generalized friction coefficient $\eta(\vec{R}, \vec{Q})$ by $M v^2 \eta(\vec{R}, \vec{Q}) = \dot{E}_{\text{n.a.}}(\vec{R}, \vec{Q})$. Here, M is the mass of the atom (in atomic mass units). The generalized coefficient $\eta(\vec{R}, \vec{Q})$ reverts to the usual friction coefficient η in the limit of slow

velocities.^{9,29,30} The energy transfer includes two qualitatively different contributions, one from the perpendicular and one from the parallel component of the atomic motion. The analysis of Eq. (2.11) for perpendicular motion was the subject of study in I. In the present study, we investigate additional effects originating from the presence of an off-normal component in the atomic trajectory. As a first step, we turn to parallel motion.

1. Parallel motion

The resonance $\epsilon_a(Z)$ and the adiabatic tunneling matrix element $V_{ka}^{(S)}(Z)$ are both constants in this case. The only time dependence enters through $\vec{R}_{\parallel}(t)$. The rate of the energy transfer is then given by

$$\begin{aligned} \dot{E}_{\parallel}(\vec{R}, \vec{Q}) &= -2 \text{Im} \sum_{ka} e^{i\theta_{k,\vec{Q}}(\vec{R})} \mathcal{G}_{a,k,\vec{Q}}^<(t, t) \\ &\times (\dot{\theta}_{k,\vec{Q}}(\vec{R}) - i\dot{Q}_{\parallel} \cdot \nabla_{\vec{k}}) V_{a,k-\vec{Q}_{\parallel}}(Z). \end{aligned} \quad (2.12)$$

This expression follows directly from Eq. (2.11) with constant Z and $\vec{Q}(t) = \vec{Q}_{\parallel}(t)$, and from the form of the matrix element $V_{a,k,\vec{Q}}(\vec{R})$ in Eq. (2.6). We note that $\dot{E}_{\parallel}(\vec{R}, \vec{Q})$ does not have any adiabatic contribution and is thus directly related to the generalized friction coefficient through $M v_{\parallel}^2 \eta_{\parallel}(\vec{R}, \vec{Q}) = \dot{E}_{\parallel}(\vec{R}, \vec{Q})$. We use the Keldysh formalism³¹ to write the Dyson equations for $\mathcal{G}_{a,k,\vec{Q}}^<(t, t')$ which, on the real time axis, become

$$\begin{aligned} \mathcal{G}_{a,k,\vec{Q}}^<(t, t') &= \int_{-\infty}^{\infty} d\tau V_{a,k,\vec{Q}_{\parallel}}^*(\vec{R}(\tau)) \{ G_k^R(t, \tau) \mathcal{G}_{a,\vec{Q}}^<(\tau, t') \\ &+ G_k^<(t, \tau) \mathcal{G}_{a,\vec{Q}}^A(\tau, t') \}. \end{aligned} \quad (2.13)$$

We insert this expression in Eq. (2.12) and obtain an expression for energy transfer in terms of the self-energies and Green's functions of the atomic level electrons,

$$\begin{aligned} \dot{E}_{\parallel}(\vec{R}, \vec{Q}) &= -2 \text{Im} \sum_a \int_{-\infty}^{\infty} d\tau \{ \tilde{K}_{a,\vec{Q}}^R(t, \tau) \mathcal{G}_{a,\vec{Q}}^<(\tau, t) \\ &+ \tilde{K}_{a,\vec{Q}}^<(t, \tau) \mathcal{G}_{a,\vec{Q}}^A(\tau, t) \}, \end{aligned} \quad (2.14)$$

where the Z dependence enters the integrand parametrically through $\epsilon_a(Z)$ and $V_{a,k,\vec{Q}}(\vec{R})$. The quantities $\tilde{K}_{a,\vec{Q}}(t, t')$ are defined by

$$\begin{aligned} \tilde{K}_{a,\vec{Q}}(t, t') &= \sum_k e^{i\theta_{k,\vec{Q}}(\vec{R})} G_k(t-t') V_{a,k,\vec{Q}_{\parallel}}^*(\vec{R}') \\ &\times [\dot{\theta}_{k,\vec{Q}}(\vec{R}) - i\dot{Q}_{\parallel} \cdot \nabla_{\vec{k}}] V_{a,k-\vec{Q}_{\parallel}}(Z), \end{aligned} \quad (2.15)$$

where $\vec{R} \equiv \vec{R}(t)$, $Z \equiv Z(t)$, and $\vec{R}' \equiv \vec{R}(t')$, and $G_k(t-t')$ is the Green's function for the bare conduction electrons. The retarded Green's function and its analytic pieces are defined in the usual way with the convention used in Ref. 32.

Equation (2.14) is the most general expressions for the electronic energy transfer between noncorrugated surfaces of simple metals and atoms moving parallel to the surface, as

long as the relevant physics is described by the Anderson model. We use Eq. (2.14) in our numerical calculations. We summarize all relevant numerical details in Sec. III C.

2. Steady state ($v_{\parallel} = \text{const}$)

If the fractional loss of the nuclear kinetic energy is small during a time short compared with the longest electronic time scale, it is reasonable to consider a simple case of constant parallel atomic velocity, i.e., $\vec{Q}_{\parallel} = \text{const}$. In this case, $\vec{Q} \cdot \nabla V_{a,\vec{k}-\vec{Q}_{\parallel}}(Z) = 0$ and $\dot{\theta}_{\vec{k},\vec{Q}}(\vec{R}) = \Theta_{\vec{k},\vec{Q}}$ is independent of time and position. Hence, the double time Green's functions and self-energies depend on the time difference only and $\dot{E}_{\parallel}(\vec{R},\vec{Q}) = \dot{E}_{\parallel}(Z,\vec{Q}_{\parallel})$. We now derive general analytic expression for the steady-state energy transfer $\dot{E}_{\parallel}(Z,\vec{Q}_{\parallel})$ in order to make connection with known results in certain limiting cases.

We first perform the Fourier transform on the right-hand side of Eq. (2.14) and use the identity for the conduction electron Green's functions,

$$G_{\vec{k}}^{\lessgtr}(\omega) = 2\pi f^{\lessgtr}(\omega) \delta(\omega - \epsilon_{\vec{k}}), \quad (2.16)$$

where $f^{<}(\omega)$ is the Fermi function and $f^{>}(\omega) = 1 - f^{<}(\omega)$. We introduce the steady-state spectral density of one-electron states $A_{a,\vec{Q}}(\omega) = -(1/\pi) \text{Im} \mathcal{G}_{a,\vec{Q}}^R(\omega)$ and write the steady-state Green's function in the form $\mathcal{G}_{a,\vec{Q}}^{<}(\omega) = 2\pi F(\vec{Q},\omega) A_{a,\vec{Q}}(\omega)$, where $F(\vec{Q},\omega) = f^{<}(\omega) + O(Q^2)$ for systems with inversion symmetry. The solution is obtained by inserting these expressions in Eq. (2.14),

$$\begin{aligned} \dot{E}_{\parallel}(\vec{R},\vec{Q}) &= \sum_a \int_{-\infty}^{\infty} d\omega \Gamma_a(\omega, Z) \\ &\times \langle \dot{\theta}_{\vec{k},\vec{Q}} [f(\omega - \dot{\theta}_{\vec{k},\vec{Q}}) - F(\vec{Q},\omega)] \rangle_{\omega} A_{a,\vec{Q}}(\omega), \end{aligned} \quad (2.17)$$

valid for interacting systems at all values of parallel velocity. The band average in Eq. (2.17) is defined by

$$\langle g(\vec{k},\vec{Q}) \rangle_{\omega} \equiv \frac{\sum_{\vec{k}} g(\vec{k},\vec{Q}) |V_{a,\vec{k}-\vec{Q}_{\parallel}}(Z)|^2 \delta(\omega - \epsilon_{\vec{k}} - \dot{\theta}_{\vec{k},\vec{Q}})}{\sum_{\vec{k}} |V_{a,\vec{k}}(Z)|^2 \delta(\omega - \epsilon_{\vec{k}})}. \quad (2.18)$$

In the limit $v_{\parallel} \rightarrow 0$, referred to here as the local friction approximation (LFA), the energy transfer assumes the linear-response form and is fully described by the equilibrium properties of the system

$$\dot{E}_{\parallel}(Z,\vec{Q}_{\parallel}) = \sum_a \int_{-\infty}^{\infty} d\omega \Gamma_a(\omega, Z) \left(-\frac{\partial f(\omega)}{\partial \omega} \right) \langle \dot{\theta}_{\vec{k},\vec{Q}}^2 \rangle_{\omega} A_a(\omega). \quad (2.19)$$

We can rewrite Eq. (2.19) by replacing the spectral function $A_a(\omega)$ and the width $\Gamma_a(\omega, Z)$ with their definitions

$$\begin{aligned} \dot{E}_{\parallel}(Z,\vec{Q}_{\parallel}) &= -2 \text{Im} \sum_a \int_{-\infty}^{\infty} d\omega \left(-\frac{\partial f(\omega)}{\partial \omega} \right) \sum_{\vec{k}} \dot{\theta}_{\vec{k},\vec{Q}}^2 V_{a,\vec{k},0}(\vec{R}) \\ &\times \mathcal{G}_a^R(\epsilon_{\vec{k}}) V_{a,\vec{k},0}^*(\vec{R}) \delta(\epsilon_{\vec{k}} - \omega), \end{aligned} \quad (2.20)$$

where we used the $\vec{Q} \rightarrow 0$ limit of the matrix elements $V_{a,\vec{k},\vec{Q}}(\vec{R})$, but kept the \vec{Q} dependence of the phase $\dot{\theta}_{\vec{k},\vec{Q}}$ because $\dot{\theta}_{\vec{k},0} = 0$ in this limit. The terms under the sum can be expressed in terms of the many-body scattering T matrix, $T_{a\vec{k},a\vec{k}'}(\omega,\vec{R}) = V_{a,\vec{k},0}(\vec{R}) \mathcal{G}_a^R(\omega) V_{a,\vec{k}',0}^*(\vec{R})$, which can in turn be written in terms of the corresponding phase shift $\delta_a(\omega, Z)$, defined by

$$T_{ka,ka} = -\frac{\sin \delta_a e^{i\delta_a}}{\rho(\omega)}. \quad (2.21)$$

However, $T_{ka,ka}$ depends on the wave vector through $\epsilon_{\vec{k}}$ only. We thus write the steady-state solution for the energy transfer in terms of the phase shift

$$\dot{E}_{\parallel}(Z,\vec{Q}_{\parallel}) = 2 \sum_a \int_{-\infty}^{\infty} \frac{d\omega}{\pi} \left(-\frac{\partial f(\omega)}{\partial \omega} \right) \langle \dot{\theta}_{\vec{k},\vec{Q}}^2 \rangle \sin^2 \delta_a(\omega, Z). \quad (2.22)$$

This formula is valid for slowly moving interacting systems and was obtained first by Yoshimori.²⁹ Equation (2.17) is a generalization of this expression. For noninteracting systems, the form of the scattering phase shift in Eq. (2.22) is known analytically,³³

$$\tan \delta_a(\omega, Z) = \frac{\Delta_a(\omega, Z)}{\omega - \epsilon_a(Z) - \Lambda_a(\omega, Z)}, \quad (2.23)$$

where $\Lambda_a(\omega, Z) \equiv P \int (d\Omega/\pi) [\Delta_a(\Omega, Z)/\omega - \Omega]$. The explicit expression for energy transfer in a noninteracting system can also be obtained directly within our formalism by expanding Eq. (2.14) in powers of velocity and keeping only the lowest term. At low velocities, the frictional force is proportional to v_{\parallel} . We discuss the validity of Eq. (2.22) in the following section. Equation (2.22) is related to the familiar expression for resistivity due to impurity scattering through a Galilean transformation.

3. General motion

When the atom moves on a general trajectory, the variations in $\epsilon_a(Z)$ as well as in the magnitude of $V_{ka}(\vec{R})$ also have to be taken into account. It is convenient to cast the expression for energy transfer as a sum of two contributions,

$$\dot{E}(\vec{R},\vec{Q}) = \dot{E}_{\perp}(\vec{R},\vec{Q}) + \dot{E}_{\parallel}(\vec{R},\vec{Q}). \quad (2.24)$$

The first term is the only contribution to $\dot{E}(\vec{R},\vec{Q})$ when the atomic trajectory is perpendicular to the surface. We write it in terms of the nonequilibrium Green's function

$$\begin{aligned} \dot{E}_\perp(\vec{R}, \vec{Q}) &= \sum_a \dot{\epsilon}_a(Z) \mathcal{G}_{a, \vec{Q}}^<(t, t) \\ &+ \sum_a \frac{\Delta(Z)}{\Delta(Z)} \operatorname{Re} \int_{-\infty}^{\infty} d\tau \{K_{a, \vec{Q}}^R(t, \tau) \mathcal{G}_{a, \vec{Q}}^<(\tau, t) \\ &+ K_{a, \vec{Q}}^<(t, \tau) \mathcal{G}_a^A(\tau, t)\} \end{aligned} \quad (2.25)$$

with the quantities $K_{a, \vec{Q}}(t, t')$ defined by

$$K_{a, \vec{Q}}(t, t') = \sum_k V_{a, \vec{k}, \vec{Q}}(\vec{R}(t)) G_k(t-t') V_{a, \vec{k}, \vec{Q}}^*(\vec{R}(t')). \quad (2.26)$$

It is formally identical with Eq. (C5) of I (Ref. 7) valid for perpendicular motion. However, its value is different, because the effect of nonzero parallel velocity enters the calculation of the Green's functions and the quantities $K_{a, \vec{Q}}(t, t')$.

We must emphasize that Eq. (2.25) is not as general as the formulas presented in the previous sections because this expression assumes the separability of $V_{a, \vec{k}, \vec{Q}}(\vec{R})$ allowing us to write $\Gamma_a(\omega, Z)$ in the form of Eq. (3.10). These additional assumptions are discussed in Sec. III C.

The second term is the only contribution to $\dot{E}_\parallel(\vec{R}, \vec{Q})$ when the atom moves parallel to the surface. It is formally identical with Eq. (2.14), but the parameters $\epsilon_a(Z)$ and $\Gamma_a(Z)$ are in general functions of time and Q_z is nonzero. Thus the two contributions to the energy transfer in Eq. (2.24) are each influenced by the other component of the velocity. We investigate the interference effects later in the paper.

III. NUMERICAL STUDIES

We now turn to the study of a more specific model, which can be solved numerically in the end. The systems we consider are open-shell atoms with either (i) one electron in an otherwise empty shell, or (ii) one hole in an otherwise full shell. We assume the shell consists of N -degenerate levels. In the discussion of the numerical results, we choose the language of electrons, i.e., the first approach here. However, the reader should keep in mind that the results from the two formulations are identical, provided that the sign of ϵ_a is also changed in going from one formulation to the other (energies are measured with respect to ϵ_F).

A. $U=0$ and $U=\infty$ limits of the theory

The first approximation we discuss relates to the interaction term in the Hamiltonian. We write the many-body term in Eq. (2.1) in terms of Coulomb repulsion $U_{aa'}$ between two electrons in states denoted by a and a' , i.e.,

$$H_{\text{int}}[Z, c_a^\dagger c_a] = \sum_{a>a'} U_{aa'}(Z) c_a^\dagger c_a c_{a'}^\dagger c_{a'}. \quad (3.1)$$

We wish to compare the theoretical predictions based on the noninteracting system ($U=0$) with those from the strongly correlated system ($U=\infty$). A noninteracting system is described by the Hamiltonian

$$\begin{aligned} H(\vec{R}) &= \sum_a \epsilon_a(Z) c_a^\dagger c_a + \sum_{ak} \epsilon_k c_{ka}^\dagger c_{ka} \\ &+ \sum_{ak} \{V_{a, \vec{k}, \vec{Q}}(\vec{R}) c_{ka}^\dagger c_a + \text{H.c.}\}. \end{aligned} \quad (3.2)$$

The noninteracting Anderson model is expected to describe accurately the physics of closed-shell atoms, where correlations play a minor role. A strongly correlated system is treated in the limit $U=\infty$. The range of validity of the $U=\infty$ model is given by the condition that U is large enough, so that only one level from the multiplet ($\epsilon_a \pm nU$, $n=0, 1, \dots, N-1$) contributes significantly to the charge and spin fluctuations. This will be the case if $|\epsilon_a \pm nU - \epsilon_F| \gg \max(T, \Gamma)$ for all but one n . Here, Γ is the width of the level and T is the temperature in energy units. It will not matter that U splits all ionization states equally or even that some may be unbound and in the continuum, because we really only use U as a device to exclude the ionization states that are far from the Fermi level and deemed to be irrelevant to the physics at hand.

We perform the $U=\infty$ limit by adopting the slave-boson technique following Coleman³⁴ and Langreth and Nordlander.³² The bosonized Hamiltonian is

$$\begin{aligned} H(\vec{R}) &= \sum_a \epsilon_a(Z) c_a^\dagger c_a + \sum_{ak} \epsilon_k c_{ka}^\dagger c_{ka} \\ &+ \sum_{ak} \{V_{a, \vec{k}, \vec{Q}}(\vec{R}) c_{ka}^\dagger b^\dagger c_a + \text{H.c.}\}. \end{aligned} \quad (3.3)$$

We use the equation of motion method of Kadanoff and Baym³⁵ to solve the Hamiltonian within the noncrossing approximation (NCA).

B. Numerical procedure

The energy transfer for strongly correlated systems is numerically obtained within the NCA. The calculation is done in two steps for both the steady state and fully dynamic conditions.

First, the auxiliary Green's functions $G_{a, \vec{Q}}$ are found self-consistently as described in the preceding subsection and in the references cited therein. In the second step, the calculated Green's functions are inserted in the expressions for $\dot{E}_\parallel(\vec{R}, \vec{Q})$ and $\dot{E}_\perp(\vec{R}, \vec{Q})$. All equations in Sec. II are entirely general and could, in principle, be used as the basis for the approximate (NCA) numerical calculations, provided the physical propagators are formed and used.

However, we write the numerical NCA solution in terms of the auxiliary Green's functions $G_{a, \vec{Q}}(t, t')$ and the NCA self-energies $\tilde{\Sigma}_{a, \vec{Q}}(t, t')$ which are identical in form with $\Sigma_{a, \vec{Q}}(t, t')$, but $K_{a, \vec{Q}}(t, t')$ is replaced by $\tilde{K}_{a, \vec{Q}}(t, t')$. The expression for $\dot{E}_\parallel(\vec{R})$ is then written in analogy with Eq. (2.14) as

$$\begin{aligned} \dot{E}_\parallel(\vec{R}, \vec{Q}) &= -2 \operatorname{Im} \sum_a \int_{-\infty}^{\infty} d\tau \{ \tilde{\Sigma}_{a, \vec{Q}}^R(t, \tau) G_{a, \vec{Q}}^<(\tau, t) \\ &+ \tilde{\Sigma}_{a, \vec{Q}}^<(t, \tau) G_{a, \vec{Q}}^A(\tau, t) \}. \end{aligned} \quad (3.4)$$

The numerical version of Eq. (2.25) is

$$\begin{aligned} \dot{E}_\perp(\vec{R}, \vec{Q}) &= \sum_a \dot{\epsilon}_a(Z) G_{a, \vec{Q}}^<(t, t) \\ &+ \sum_a \frac{\Delta(Z)}{\Delta(Z)} \text{Re} \int_{-\infty}^{\infty} d\tau \{ \sum_{a, \vec{Q}}^R G_{a, \vec{Q}}^<(t, \tau) G_{a, \vec{Q}}^<(\tau, t) \\ &+ \sum_{a, \vec{Q}}^< G_{a, \vec{Q}}^A(\tau, t) \}. \end{aligned} \quad (3.5)$$

We conclude this section by defining the model used in the numerical calculations.

C. Model-specific assumptions and parametrizations

For the purpose of the numerical calculations we make additional approximation and specify our model system. First, we neglect the contribution to energy transfer from the term $[\dot{\vec{Q}}_\parallel \cdot \nabla_{\vec{k}} V_{a, \vec{k} - \vec{Q}_\parallel}(Z)]$, which arises from the force on the electrons moving with the atom due to the atomic acceleration. Since $V_{a, \vec{k} - \vec{Q}_\parallel}(Z)$ is typically a slowly varying function of \vec{k} near the Fermi surface, this is a reasonable approximation unless $|\dot{\vec{Q}}_\parallel| \gg |\vec{Q}_\parallel|$ when this term might dominate. This condition occurs any time the atomic motion reverses its direction, e.g., oscillations.

We are mainly interested in assessing the effect of the atom velocity on the Kondo induced electronic friction. Since the formation of the Kondo resonance is affected on the scale, $Qk_F \sim \gamma \ll 1$,²⁸ where γ is the width of the many-body resonance at the Fermi level. Since $k_F \sim 1$, it is sufficient to limit our theory to velocities much smaller than the Fermi velocity, i.e., $Q \ll k_F$. In such a case, a simplified interaction matrix can be used. We have discussed these assumptions and approximations systematically in Ref. 28. Here, we only summarize them: (i) the phase $\theta_{\vec{k}, \vec{Q}}$ includes contributions from both the parallel and perpendicular components of the ion velocity. We only retain terms of the lowest order in velocity and write $\theta_{\vec{k}, \vec{Q}} = -\vec{k} \cdot \vec{R}_\parallel$; (ii) we neglect the effects of \vec{Q}_\parallel in the magnitude of the matrix element and write $V_{a, \vec{k} - \vec{Q}_\parallel}(Z) \rightarrow V_{a, k}^{(S)}(Z)$; (iii) finally, we neglect the anisotropy of $V_{a, k}^{(S)}$ and assume the k dependence comes only in the form of ϵ_k . The matrix element becomes

$$V_{a, \vec{k}, \vec{Q}}(\vec{R}) = e^{-i\vec{k}_\parallel \vec{R}} V_{a, \epsilon_k}^{(S)}(Z). \quad (3.6)$$

Here, $V_{a, \epsilon_k}^{(S)}(Z)$ is the matrix element defined in Ref. 37 and considered in I.⁷

We also assume the energy dependence of $V_{a, \epsilon_k}^{(S)}(Z)$ is time invariant. In this case, the potential is separable, $V_{a, \epsilon_k}^{(S)}(Z) \equiv u(Z) v(\epsilon_k)$. The full width of the atomic level defined in Eq. (2.10) becomes

$$\Gamma(\omega, Z) = 2\pi\rho(\omega)u^2(Z)v^2(\omega), \quad (3.7)$$

where $\rho(\omega) = \sum_k \delta(\omega - \epsilon_k)$ is the density of states. We can also express $\Gamma(\omega, Z)$ in terms of the Fermi-level width $\Gamma(0, Z)$. To this end, we introduce a function

$$\kappa(\omega) = \frac{\rho(\omega)v(\omega)}{\rho(0)v(0)}. \quad (3.8)$$

We use a parabolic band with $\kappa(\omega) = (1 - \omega^2/D^2)$ for $|\omega| < D$ and zero otherwise, and the band half-width $D = 5$ eV. We take the band to be half filled. Different choices of $\kappa(\omega)$ and D produce only quantitative differences. The Fermi-level half-width parameter $\Delta(Z) = \frac{1}{2}\Gamma(0, Z)$ is used as an input parameter in our calculations along with $\epsilon_a(Z)$ and k_F . Since the atom-metal interaction is proportional to the wavefunction overlap, we parametrize Δ by an exponential dependence on the distance from the surface,

$$N\Delta(Z) = \Delta_0 e^{-bZ}. \quad (3.9)$$

Here, N is the degeneracy of the atomic level ϵ_a . The width in Eq. (3.7) can thus be written in the form

$$\Gamma(\omega, Z) = 2\kappa(\omega)\Delta(Z). \quad (3.10)$$

The electronic level $\epsilon_a(Z)$ is assumed to shift due to the interaction with the metal surface. With the exception of very small separation, the shift is controlled by the image potential. We use a model in which the electronic state ϵ_a corresponds to the ionization level of the atom and write

$$\epsilon_a(Z) = \epsilon_\infty + \frac{1}{4|Z-1|}. \quad (3.11)$$

The opposite sign would appear in the expression for an affinity level.

Given the explicit form of the interaction $V_{a, \epsilon_k}^{(S)}(Z)$ and of the bare conduction-band electron propagator $G_k(t-t')$, we can write the analytic pieces of $K_{a,0}(t, t')$ and $\tilde{K}_{a,0}(t, t')$ in terms of the quantities defined above as

$$K_{a,0}^{\cong}(t, t') = 2\sqrt{\Delta(Z(t))\Delta(Z(t'))}f^{\cong}(t, t') \quad (3.12)$$

with the effect of nonzero parallel velocity incorporated entirely in the definition of $f^{\cong}(t, t')$,

$$f^{\cong}(t, t') = \int \frac{d\omega}{2\pi} \kappa(\omega) f^{\cong}(\omega) e^{-i\omega(t-t')} \langle e^{i\vec{k}_\parallel[\vec{R}(t) - \vec{R}(t')]} \rangle_\omega \quad (3.13)$$

and

$$\tilde{K}_{a,0}^{\cong}(t, t') = 2\sqrt{\Delta(Z(t))\Delta(Z(t'))}\tilde{f}^{\cong}(t, t') \quad (3.14)$$

with

$$\begin{aligned} \tilde{f}^{\cong}(t, t') &= k_F^{-1} \int_{-\infty}^{\infty} \frac{d\omega}{2\pi} \kappa(\omega) f^{\cong}(\omega) e^{-i\omega(t-t')} \\ &\times \langle k_\parallel e^{i\vec{k}_\parallel[\vec{R}(t) - \vec{R}(t')]} \rangle_\omega, \end{aligned} \quad (3.15)$$

where the averages are evaluated in Appendix B for a band with a parabolic dependence of ϵ_k on the wave vector.

All numerical results presented here were obtained with the parametrization of the atomic level position according to Eq. (2.2) with $\epsilon_\infty = -0.125$ a.u. The half-width is parametrized with Eq. (3.9), with $\Delta_0 = 0.75$ and $b = 0.65$ all in atomic units. We keep $N\Delta$ constant for systems with different degeneracy N . Provided the N -degenerate level is nearly fully

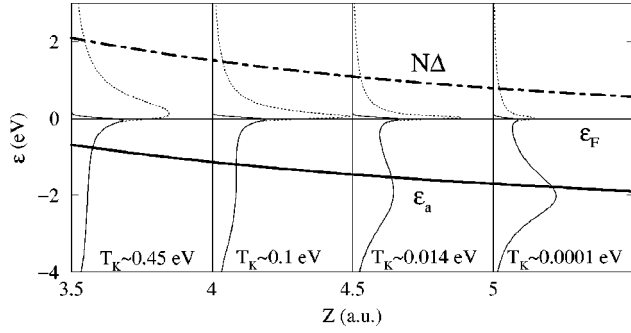


FIG. 1. Parametrization of the atom-induced resonance and the equilibrium local electronic structure is shown for several atom-metal separations Z . The dotted lines correspond to the total density of states and the solid lines to the density of occupied states. The degeneracy is $N=2$, $T=0.001$ hartree, and $k_F=0.8$ a.u.

occupied, this ensures nearly the same tunneling rate and level width for such atoms as would be determined, for example, from photoemission experiments. In addition to the two Newns parameters, the solution in the presence of non-zero parallel velocity involves an additional parameter k_F , the Fermi wave vector, which enters through the band averages in f^{\approx} and \tilde{f}^{\approx} . We used the value $k_F=0.8$ a.u. in all the results shown.

IV. RESULTS

We show the parametrization of ϵ_a and $N\Delta$ in Fig. 1. We also plot, for several atom-surface separations, the equilibrium spectral density for an $N=2$ interacting ($U=\infty$) system at $T=0.001$ hartree (~ 316 K). The dotted lines show the total spectral density and the solid lines show the occupied density of states. In the local moment regime considered here, the spin-flip scattering of substrate electrons (holes) with the uncompensated spin on the atom provides an additional hybridization channel, which lowers the energy of the atom-metal complex. The system then has a tendency to maximize the rate of low-energy scattering by rearranging its electronic structure, so that the Φ number of available states near the Fermi energy is increased. This takes the form of a sharp resonance (the Kondo resonance) in the local density of states at the atom which appears near the Fermi level as seen in Fig. 1. The corresponding Kondo temperature T_K at the given distance Z are shown on the bottom of the figure. The estimates of Kondo temperature used throughout this paper are based on the Bethe ansatz³⁸ formula for the low-energy scale (called T_I in Ref. 38),

$$T_K = \Gamma \left(1 + \frac{1}{N} \right) D_r \left(\frac{N\Delta}{\pi D_r} \right)^{1/N} \exp \left(- \frac{\pi |\epsilon|}{N\Delta} \right), \quad (4.1)$$

where Γ is the gamma function and $D_r = e^{-1/2} D$ is rescaled³⁷ for the assumed parabolic shape of $\xi(\epsilon)$. The Kondo temperatures in the atom surface can vary over a large range of values as the adsorbates move with respect to the surface. For known Kondo systems, the Kondo temperatures are expected to be lower at surfaces due to the smaller adsorbate widths compared to their bulk values. On the other hand, new Kondo systems, such as possibly Ca/Cu, can form at surfaces with T_K at room temperature or higher.⁶ Based on

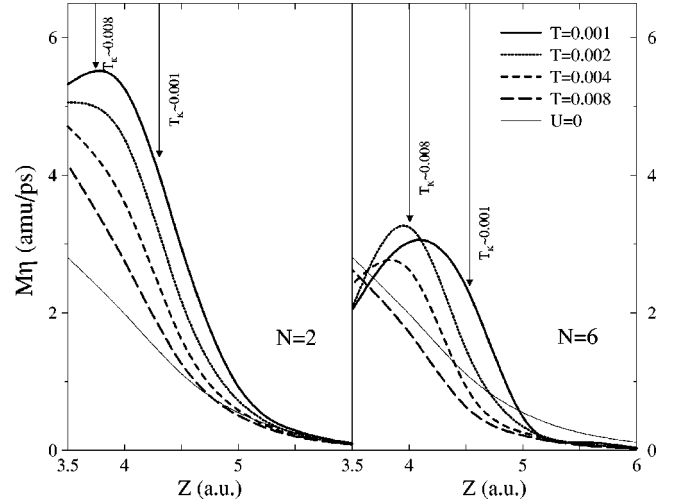


FIG. 2. Electronic friction coefficient $M\eta$ in the $v_{\parallel} \rightarrow 0$ limit (LFA) vs the atom-metal separation Z for parallel motion along smooth surface. Each curve corresponds to a different temperature T . The $N=2$ and $N=6$ interacting models and the noninteracting ($U=0$) model are shown.

two-photon photoemission experiments,⁴⁰ Yoshimori estimated NO/Cu(111) (Ref. 39) to be a Kondo system with $T_K \sim 8$ K.

A. Parallel motion, $v_{\parallel} = \text{const}$

In this section, we present our calculations of electronic friction for atoms moving at constant speed, v_{\parallel} , parallel to the surface. The friction coefficient η is then independent of time and can be expressed in terms of the steady-state properties of the system. The energy transfer at constant parallel speed will prove useful to consider for systems in which the change in speed is small on the longest characteristic electronic time scales τ , i.e., for $F\tau/Mv < 1$. Here M is the atomic mass and F is the frictional force.

We show in Fig. 2 the friction coefficient $M\eta \equiv \dot{E}/v^2$ in the LFA limit ($v_{\parallel} \rightarrow 0$) for the parametrization [Eqs. (3.9) and (3.11)] as a function of Z . We compare results for the strongly correlated system at several temperatures with that for the noninteracting system. We see a strong enhancement of the friction in a region that coincides with the existence of the Kondo resonance. We found in a previous work^{7,41} that the maximum enhancement occurs near the position Z where $T_K(Z) \sim T$ in the case of atoms moving perpendicular to the surface. A quantitative difference between the two cases exists. The Kondo enhancement in the parallel motion is much smaller than it is for realistic parametrization of the perpendicular motion.⁴¹ As a consequence, the maximum friction experienced by atoms moving along the surface occurs closer to the Fermi-level crossing (here at $z=3$ a.u.) than the condition $T_K(Z) \sim T$ would indicate. As the temperature is increased, the Kondo resonance broadens and the enhancement of electronic friction due to the correlation effects weakens.

In the case of parallel motion, we find qualitatively different behavior of the friction with the degeneracy N [Fig. 2(a) and Fig. 2(b)]. Unlike in the case of perpendicular motion, where the Kondo enhancement of electronic friction

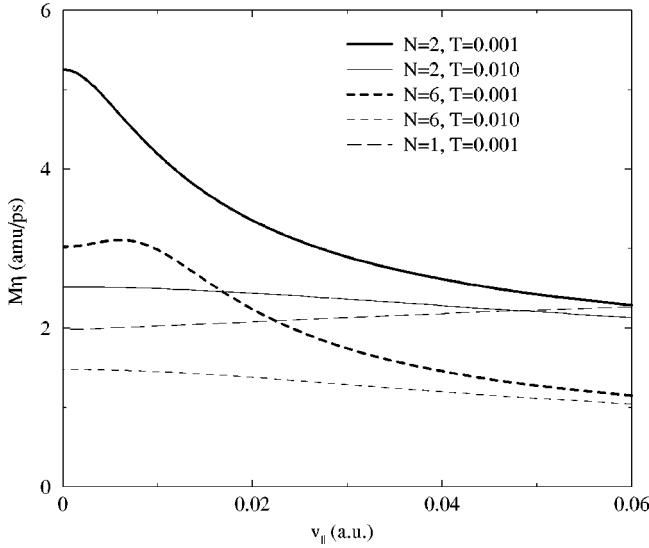


FIG. 3. Electronic friction coefficient $M\eta$ vs v_{\parallel} at $Z=4.5$ a.u. We show the $N=2$ and $N=6$ interacting models at different temperatures and the noninteracting model ($N=1$).

was stronger at larger N , we find the opposite relation between the friction η and the degeneracy N . This is manifested by comparing the right and left panels of Fig. 2. The different behavior can be understood by the following argument.

According to Eq. (2.19), the friction is, at low enough temperatures, given by $2k_F^2(N\Delta(Z))A_a(\epsilon_F)$, assuming each of the N atomic levels a has the same width and spectral function. The parameter $N\Delta(Z)$, an input parameter in our calculations, is kept constant for different degeneracies. This choice ensures that the tunneling rate and the atomic level width are independent of N in the Kondo regime where the level occupation $\langle n \rangle = N \int d\omega f^<(\omega) A_a(\omega)$ is almost 1. Thus the friction is essentially given by a product of N -independent quantities and the spectral density of states $A_a(\epsilon_F)$ for electrons in level a . The total density of electron states at the Fermi level, $\rho(\epsilon_F) = NA_a(\epsilon_F)$, increases with N because the spectral weight shifts away from the broad resonance at ϵ_a into the Kondo resonance at ϵ_F . However, the density of states associated with a particular level a , i.e., $A_a(\epsilon_F)$, decreases with degeneracy N . This explains the trend in Fig. 2.

We now turn to energy transfer at finite parallel velocities. We summarize our results in Fig. 3. We show the friction coefficient $M\eta$ for the $N=2$ and $N=6$ interacting systems at two temperatures $T=0.001$ and $T=0.01$ hartree, and for the noninteracting ($N=1$) system at $T=0.001$ for $Z=4.5$ a.u. We only show one temperature for the $U=0$ model because the friction exhibits very little temperature dependence in this range. At small v_{\parallel} , the friction converges to a constant value provided by the LFA limit. The main effect of v_{\parallel} is the deviation of the friction coefficient η from its LFA limit at velocities $k_F v_{\parallel} \sim \Gamma$, where Γ is the width of the narrowest feature in the electronic structure.

The correlated systems ($N=2$ and $N=6$) show the interplay between the two electronic time scales involved. Deviations from the LFA values begin to appear at much smaller v_{\parallel} than in the noninteracting system, and the dependence of friction on the parallel velocity is nontrivial. Two effects

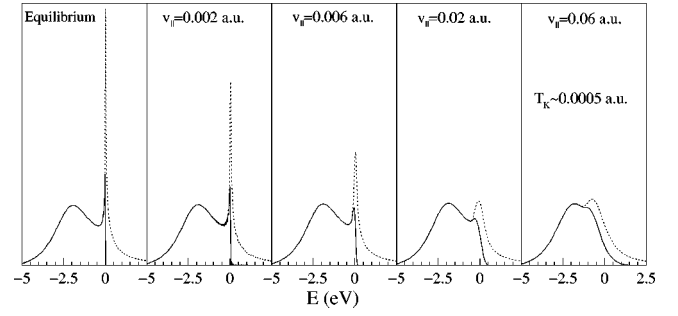


FIG. 4. Spectral function for different atomic velocities v_{\parallel} of an atom moving parallel to the surface at a distance $Z=4.5$ a.u. The dotted line corresponds to the total density of states and the solid line to the density of occupied states for $T=100$ K, $N=2$, and $k_F=0.8$ a.u.

contribute. The Kondo peak broadening, which occurs at parallel velocities $v_{\parallel} k_F \sim \gamma$ (the width of the Kondo resonance), leads to the decrease in $M\eta$ when velocities reach this order of magnitude. This effect is counteracted by the kinetic population of the resonance. We see the effect of kinetic population best for $N=6$ at $T=100$ K, where the friction initially increases with v_{\parallel} . The reason why the increase is present in $N=6$ but not in $N=2$ can be understood in term of the spectral weight of the Kondo peak, which is larger in the $N=6$ system. The kinetic excitations into the Kondo resonance—always near the Fermi level—initially outweighs the effect of the Kondo resonance broadening. We demonstrate the behavior of the spectral function versus v_{\parallel} in Fig. 4, where we show the steady-state spectral functions at different atom velocities for $Z=4.5$ a.u. The density of states for velocities up to $v_{\parallel}=0.001$ a.u., is virtually indistinguishable from the equilibrium DOS. The effects of parallel velocity on the Kondo resonance are apparent at $v_{\parallel}=0.002$ a.u., where $v_{\parallel} k_F > T_K$.

The behavior of the spectral functions in Fig. 4 can be explained as follows. When the atom moves along the surface, the system is out of equilibrium by virtue of the changing phase of the potential $V_{ka}(\vec{R}(t))$. The Kondo resonance forms on time scales comparable with the inverse of its width. The frequency of oscillations in the phase of the potential $V_{ka}(\vec{R}(t))$ is $\omega = v_{\parallel} k_F$. As the frequency increases and becomes comparable with the Kondo peak width, formation of the resonance is adversely affected by the motion. The Kondo peak is smeared out by the apparent broadening of the Fermi surface as electrons moving parallel and antiparallel to the atom motion appear to have different k_F . The width of the Kondo resonance thus has a lower bound given by the frequency ω . At the same time, the electron population is seen to be kinetically excited above ϵ_F . Different values of k_F rescale the frequency ω at a given velocity.

B. General direction, $v_{\parallel} = \text{const}$

In this section we discuss the energy transfer in the case of a more general trajectory. In particular, we address the question of the interference between the parallel and normal directions. We can write the energy transfer formally as a sum of three terms,

$$\dot{E}(\vec{R}, \vec{Q}) = \dot{E}_{\parallel}(\vec{R}, \vec{Q}_{\parallel}) + \dot{E}_{\perp}(\vec{R}, \vec{Q}_{\perp}) + \text{interference}. \quad (4.2)$$

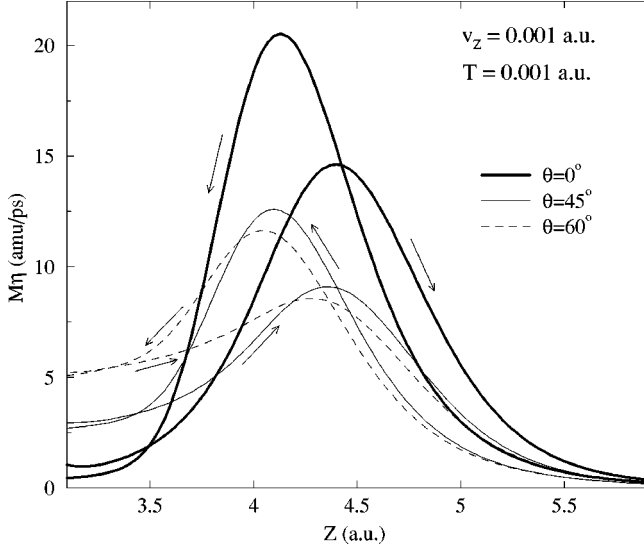


FIG. 5. Electronic friction coefficient $M\eta$ as a function of scattering angle for $N=2$ and at $v_z=T=0.001$ a.u. The arrows indicate the direction of atomic motion.

Here, $\dot{E}_\perp(\vec{R}, \vec{Q}_\perp)$ is the perpendicular component given by Eq. (3.5) and evaluated for $\vec{Q}=(0, Q_z)$. The parallel component $\dot{E}_\parallel(\vec{R}, \vec{Q}_\parallel)$ is given by Eq. (3.4) evaluated at a distance given by the position \vec{R} and assuming $\vec{Q}=(\vec{Q}_\parallel, 0)$ at that time. The interference term is equal to the difference between the total energy transfer and the two contributions. It is important to ask whether the interference term can be large under certain scattering geometries and whether it can alter the conclusions of the analysis presented here and in I. It is certainly possible that an atom moving at an angle θ with respect to the normal to the surface will no longer suffer the friction enhancements found in I. This can happen because the Kondo resonance is destroyed by large \dot{v}_\parallel ; see Fig. 4.

We find the interference term small under all experimentally relevant conditions. However, as Fig. 5 demonstrates, the parallel velocity has an effect on $\dot{E}_\perp(t)$ equivalent to raising the electronic temperature with $k_F v_\parallel \sim T$. Nevertheless, significant Kondo enhancement of electronic friction persists for angles as large as 60° .

V. CONCLUSIONS

We studied the effect of intra-atomic Coulomb correlations on electronic friction experienced by atoms or molecules moving near a metal surface. We evaluated the effect of the off-normal component of atomic motion on the Kondo enhancement predicted in I.

We have shown that magnetic atoms moving near metal surfaces experience friction that could be significantly larger than that predicted by the traditional noninteracting theory. The Kondo enhancements are not as large for atoms moving parallel to the surface as they can be in the case of perpendicular motion. The maximum enhancement occurs at a distance from the surface where the Kondo temperature T_K is of the same order of magnitude as the temperature of the band electrons. The friction is also strongly position dependent. At low velocities, the friction force $F_f = M\eta v$ is proportional to

the velocity. However, as the kinetic energy of the nuclei increases, the friction η itself depends on velocities and deviations from the linearity appear. The velocity at which the LFA breaks down is generally much lower if the strongly correlated mixed valent and Kondo states are important. The deviations from the LFA occur when $k_F v_\parallel \sim \gamma$, where γ is the width of the Kondo resonance. Since the Kondo peak is much narrower than the level width, Γ , the effect of parallel velocity is felt much sooner by the correlated system. The strong and anomalous temperature dependence of the friction in the Kondo regime should provide the experimental signature for the effects studied here.

APPENDIX A: GREEN'S FUNCTIONS IN THE PRESENCE OF NONZERO PARALLEL VELOCITY

The method for solving the NCA equations has been described elsewhere both for the equilibrium³⁶ and the nonequilibrium^{32,37} situations. We refer the reader to these papers for details. In this appendix, we outline the generalization of the theory due to the nonzero parallel velocity and we summarize the most important steps and formulas.

The equations of motion are written in terms of the auxiliary Green's functions of NCA. The Green's function for the level a is $G_{a,\vec{Q}}(t,t') = -i\langle T_C c_a(t) c_a^\dagger(t') \rangle_{\vec{Q}}$ and for the slave boson $B_{\vec{Q}}(t,t') = -i\langle T_C b(t) b^\dagger(t') \rangle_{\vec{Q}}$. The physical propagator for the electrons in the atomic level ϵ_a is, within the NCA approximation, given by $\mathcal{G}_{a,\vec{Q}}(t,t') = -i\langle T_C \alpha_a(t) \alpha_a^\dagger(t') \rangle_{\vec{Q}}$, where $\alpha_a(t) = b^\dagger(t) c_a(t)$ and the symbol T_C orders the operators according to their position on a contour C in the complex time plane.^{35,31} The effect of the parallel velocity enters the modified self-energies expressed in terms of the quantities $K_{a,\vec{Q}}(t,t')$ defined in Eq. (2.26). The self-energy of the noninteracting system is identical with $K_{a,\vec{Q}}(t,t')$. The NCA expressions for the self-energies of the atomic level electrons are

$$\Sigma_{a,\vec{Q}}^{\cong}(t,t') = K_{a,\vec{Q}}^{\cong}(t,t') B_{\vec{Q}}^{\cong}(t,t'), \quad (\text{A1})$$

$$\Sigma_{a,\vec{Q}}^{R,A}(t,t') = K_{a,\vec{Q}}^{>}(t,t') B_{\vec{Q}}^{R,A}(t,t'), \quad (\text{A2})$$

and the slave boson self-energies are

$$\Pi_{\vec{Q}}^{\cong}(t,t') = \sum_a K_{a,\vec{Q}}^{\cong}(t',t) G_{a,\vec{Q}}^{\cong}(t,t'), \quad (\text{A3})$$

$$\Pi_{\vec{Q}}^{R,A}(t,t') = \sum_a K_{a,\vec{Q}}^{<}(t',t) G_{a,\vec{Q}}^{R,A}(t,t'). \quad (\text{A4})$$

The coupled equations of motion are then solved with these modified self-energies in exactly the same way as discussed in Ref. 37.

In the steady state $\vec{R}_\parallel(t) - \vec{R}_\parallel(t') = \vec{Q}_\parallel(t - t')$, and the self-energies depend on the time difference only. The system is thus described in terms of time-independent Green's functions. We can write their solution in a standard way,

$$\mathcal{G}_{a,\vec{Q}}^{R,A}(\omega) = [\omega - \epsilon - \Sigma_{a,\vec{Q}}^{R,A}(\omega)]^{-1} \quad (\text{A5})$$

and

$$\mathcal{G}_{a,\tilde{Q}}^{\lessdot}(\omega) = \mathcal{G}_{a,\tilde{Q}}^R(\omega) \Sigma_{a,\tilde{Q}}^{\lessdot}(\omega) \mathcal{G}_{a,\tilde{Q}}^A(\omega). \quad (\text{A6})$$

Given the appropriate form of the self-energies, the last two equations represent model-independent expressions. However, care must be exercised in writing the equivalent expression within NCA. The two equations are still valid assuming the physical propagator $\mathcal{G}_{a,\tilde{Q}}(\omega)$ is everywhere replaced by the auxiliary one $G_{a,\tilde{Q}}(\omega)$ and NCA self-energies are used. In order to obtain a self-consistent NCA solution, we also need the auxiliary slave boson propagators

$$B_{\tilde{Q}}^{R,A}(\omega) = [\omega - \Pi_{\tilde{Q}}^{R,A}(\omega)]^{-1} \quad (\text{A7})$$

and

$$B_{\tilde{Q}}^{\lessdot}(\omega) = B_{\tilde{Q}}^R(\omega) \Pi_{\tilde{Q}}^{\lessdot}(\omega) B_{\tilde{Q}}^A(\omega). \quad (\text{A8})$$

The solution of the coupled steady-state equations is then formally identical with the equilibrium solution discussed in Brunner and Langreth³⁶ with the modified self-energies defined here.

APPENDIX B: EXPLICIT FORM OF THE BAND AVERAGES

In this appendix, we show the calculation of the band averages appearing in the text. For this purpose, we make a further assumption that the magnitude of the atom-metal interaction depends on the wave vector only through the band energy, i.e., $V_{ka}(Z) = V_{\epsilon_k a}(Z)$. In this case, the potential can be taken out of the sum in the definition (2.18) and we can write

$$\langle f(k_x) \rangle \equiv \frac{\sum_k f(k_x) \delta(\omega - \epsilon_k)}{\sum_k \delta(\omega - \epsilon_k)}. \quad (\text{B1})$$

We will also assume a simple parabolic dependence of the band energies on wave vector \vec{k} , i.e., $\epsilon_k = k^2/2m^*$, where m^*

is the effective mass of the band electrons and the energy is measured from the bottom of the band. We remind the reader that all energies in the other parts of the paper are measured from ϵ_F . We define a wave vector $q = \sqrt{2m^* \omega}$ of an electron with energy ω , and the Fermi wave vector $k_F = \sqrt{2m^* \epsilon_F}$. Using our convention of $\epsilon_F = 0$ with the band of width D , the relation between q and k_F is expressed as $q = k_F \sqrt{1 + \omega/D}$.

For the above model of electron energies, simple calculations yield

$$\sum_k \delta(\omega - \epsilon_k) = \frac{qV}{2\pi^2}, \quad \sum_k k_x^2 \delta(\omega - \epsilon_k) = \frac{q^3 V}{6\pi^2}, \quad (\text{B2})$$

and

$$\sum_k e^{ik_x X} \delta(\omega - \epsilon_k) = \frac{V}{2\pi^2 X} \sin(qX). \quad (\text{B3})$$

The band average in Eq. (3.13) is then

$$\langle e^{ik_x X} \rangle = \frac{\sin(qX)}{qX}. \quad (\text{B4})$$

The average in Eq. (3.15) is obtained by differentiating the last equation with respect to X and is

$$\langle k_x e^{ik_x X} \rangle = \frac{i}{X} \left\{ \frac{\sin(qX)}{qX} - \cos(qX) \right\}. \quad (\text{B5})$$

Finally, the average appearing in Eq. (2.19) is

$$\langle \xi_x^2 \rangle = \frac{1}{3} \left(1 + \frac{\omega}{D} \right). \quad (\text{B6})$$

For the parabolic band, we can also write an explicit expression for $\Lambda(\omega, Z)$ which was defined below Eq. (2.23),

$$\Lambda(\omega, Z) = \Delta(Z) \left(2 \frac{\omega}{D} + \kappa(\omega) \ln \frac{D + \omega}{D - \omega} \right). \quad (\text{B7})$$

-
- ¹V. Madhavan *et al.*, Science **280**, 567 (1998).
²J. Li, W. D. Schneider, R. Berndt, and B. Delley, Phys. Rev. Lett. **80**, 2893 (1998).
³A. C. Hewson, *The Kondo Problem to Heavy Fermions* (Cambridge University Press, Cambridge, 1993).
⁴E. Müller-Hartmann, T. V. Ramakrishnan, and G. Toulouse, Phys. Rev. B **3**, 1102 (1971).
⁵H. Shao, P. Nordlander, and D. C. Langreth, Phys. Rev. Lett. **77**, 948 (1996).
⁶J. Merino and J. B. Marston, Phys. Rev. B **58**, 6982 (1998).
⁷M. Plihal and D. C. Langreth, Phys. Rev. B **58**, 2191 (1998).
⁸K. P. Bohnen, M. Kiwi, and H. Suhl, Phys. Rev. Lett. **34**, 1512 (1975).
⁹A. Nourtier, J. Phys. (Paris) **38**, 479 (1977).
¹⁰B. N. J. Persson and M. Persson, Solid State Commun. **36**, 175 (1980).
¹¹R. Ryberg, Phys. Rev. B **32**, 2671 (1985).
¹²C. J. Hirschmugl, G. P. Williams, F. M. Hoffmann, and Y. J. Chabal, Phys. Rev. Lett. **65**, 480 (1990).
¹³Z. Crljen and D. C. Langreth, Phys. Rev. B **35**, 4224 (1987).
¹⁴A. I. Volokitin and B. N. J. Persson, Phys. Rev. B **52**, 2899 (1995).
¹⁵J. C. Tully, M. Gomez, and M. Head-Gordon, J. Vac. Sci. Technol. A **11**, 1914 (1993).
¹⁶T. T. Rantala and A. Rosen, Phys. Rev. B **34**, 837 (1986).
¹⁷M. Head-Gordon and J. C. Tully, J. Chem. Phys. **96**, 3939 (1992).
¹⁸J. A. Prybyla *et al.*, Phys. Rev. Lett. **64**, 1537 (1990).
¹⁹J. A. Prybyla, H. W. K. Tom, and G. D. Aumiller, Phys. Rev. Lett. **68**, 503 (1992).
²⁰J. W. Gadzuk *et al.*, Surf. Sci. **235**, 317 (1990).
²¹S. Gao, M. Persson, and B. I. Lundqvist, Solid State Commun. **84**, 271 (1992).
²²R. E. Walkrup, D. M. Newns, and P. Avouris, Phys. Rev. B **48**, 1858 (1993).
²³D. M. Eigler, C. P. Lutz, and W. E. Rudge, Nature (London) **352**, 600 (1991).

- ²⁴B. C. Stipe *et al.*, Phys. Rev. Lett. **78**, 4410 (1997).
- ²⁵S. Gao, M. Persson, and B. I. Lundqvist, Phys. Rev. B **55**, 4825 (1997).
- ²⁶B. N. J. Persson, Phys. Rev. B **48**, 18 140 (1993).
- ²⁷A. Dayo, W. Alnasrallah, and J. Krim, Phys. Rev. Lett. **80**, 1690 (1998).
- ²⁸M. Plihal, D. C. Langreth, and P. A. Norlander, Phys. Rev. B **59**, 13 322 (1999).
- ²⁹A. Yoshimori and J. Motchane, J. Phys. Soc. Jpn. **51**, 1826 (1982).
- ³⁰M. Brandbyge *et al.*, Phys. Rev. B **52**, 6042 (1995).
- ³¹L. V. Keldysh, Zh. Eksp. Teor. Fiz. **47**, 1515 (1964), [Sov. Phys. JETP **20**, 1018 (1965)].
- ³²D. C. Langreth and P. Norlander, Phys. Rev. B **43**, 2541 (1991).
- ³³A. Blandin, A. Nourtier, and D. Hone, J. Phys. (Paris) **37**, 369 (1976).
- ³⁴P. Coleman, Phys. Rev. B **29**, 3035 (1984).
- ³⁵L. P. Kadanoff and G. Baym, *Quantum Statistical Mechanics* (Benjamin, New York, 1962).
- ³⁶T. Brunner and D. C. Langreth, Phys. Rev. B **55**, 2578 (1997).
- ³⁷H. Shao, D. C. Langreth, and P. Norlander, Phys. Rev. B **49**, 13 929 (1994).
- ³⁸J. W. Rasul and A. C. Hewson, J. Phys. C **17**, 3337 (1984).
- ³⁹A. Yoshimori, Surf. Sci. **342**, L1101 (1995).
- ⁴⁰I. Kinoshita, A. Misu, and T. Munakata, J. Chem. Phys. **102**, 2970 (1995).
- ⁴¹M. Plihal and D. C. Langreth, Surf. Sci. Lett. **395**, 252 (1998).